



Original Article

Study on promoting the regeneration of grafted fat by cell-assisted lipotransfer

Hongtao Fu ^a, Shanshan Dong ^b, Kun Li ^{c,*}^a Department of Breast Surgery, The First Affiliated Hospital with Nanjing Medical University, Nanjing 210029, China^b Department of Medicine, Hunan Cancer Hospital/the Affiliated Cancer Hospital of Xiangya School of Medicine, Central South University, China^c Department of Emergency Medicine, The Affiliated Changsha Central Hospital, Hengyang Medical School, University of South China, NO. 161 Shaoshan South Road, Changsha 410004, Hunan, China

ARTICLE INFO

Article history:

Received 23 September 2022

Received in revised form

10 November 2022

Accepted 23 November 2022

Keywords:

Autologous fat grafting

Adipose-derived stromal/stem cells

Fibroblasts

Cell-assisted lipotransfer

ABSTRACT

Background: Cell-assisted lipotransfer (CAL), a modified adipose-derived stromal/stem cells (ADSCs)-based approach for autologous fat grafting that is an ideal option for soft tissue augmentation, has many shortcomings in terms of retention and adverse effects. The objective of our study was to improve the treatment efficacy of CAL by adding fibroblasts.

Methods: ADSCs and fibroblasts were isolated from human adipose and dermal tissues, with fibroblasts identified by immunofluorescence and ADSCs identified by the multilineage differentiation method. We performed cell proliferation, apoptosis, migration, adipogenic, and hemangioendothelial differentiation experiments, qPCR and Western blotting analysis in co-cultures of fibroblasts and ADSCs. Subsequently, we conducted animal experiments with BALB/c nude mice. Masson's staining, immunofluorescence staining and ultrasound were used to analyze the occurrence of adverse reactions of the grafted fat, and CT and three-dimensional reconstruction were used to accurately evaluate the volume of the grafted fat.

Results: We found that the co-culture of fibroblasts and ADSCs promoted their mutual proliferation, adipogenic differentiation, hemangioendothelial differentiation and proliferation and migration of HUVECs. Fibroblasts inhibit the apoptosis of ADSCs. Moreover, in animal experiments, the autografted adipose group combined with ADSCs and fibroblasts had the least occurrence of oily cysts, and fat had the best form of survival.

Conclusions: We enhanced adipocyte regeneration and angiogenesis in ADSCs and fibroblast cells after adding fibroblasts to conventional CAL autologous fat grafts. In turn, the volume retention rate of the grafted fat is improved, and the adverse reactions are reduced.

© 2022, The Japanese Society for Regenerative Medicine. Production and hosting by Elsevier B.V. This is an open access article under the CC BY-NC-ND license (<http://creativecommons.org/licenses/by-nc-nd/4.0/>).

1. Introduction

Breast cancer is the most common malignant tumor in the world, and its global burden exceeds all other cancers [1,2]. After breast cancer surgery, the quality of life of breast cancer patients is influenced by partial breast deformity, which is disfiguring and can stigmatize the patient [2]. To improve their quality of life, up to 40% of women diagnosed with breast cancer require breast reconstruction as a surgical treatment [3]. Female patients who choose breast reconstruction range from implants (usually saline or silicone) to

autologous tissues [4,5]. However, exponentially increasing evidence has shown that breast implants are associated with serious complications, such as capsular contracture, infection, lump, implant rupture, squeeze (implant penetrates the skin) [5–8] and anaplastic large cell lymphoma [7]. These complications cast a shadow on the future of implant-based breast augmentation surgery. Autologous tissues for breast reconstruction include free flaps and autologous fat. Compared to breast implants, free flaps look and feel more natural and more like natural breast tissue [9]. There is no risk of breast implant rupture, but the disadvantages of using free flaps include longer surgery and hospital stay, higher donor site morbidity (e.g., abdominal bulging and scarring), vascular flap complications, etc [10,11].

Autologous fat seems to be a promising option for breast reconstruction. It is being accepted as an ideal soft-tissue filler because it is biocompatible, versatile (such as body shaping),

* Corresponding author. The Affiliated Changsha Central Hospital, 161 Shaoshan South Road, Changsha 410004, China.

E-mail address: kunli666003@163.com (K. Li).

Peer review under responsibility of the Japanese Society for Regenerative Medicine.

nonimmunogenic, and easily available [12]. However, the reabsorption rate of grafted fat is highly unpredictable and has been reported to range from 20 to 90% [13]. Therefore, the outcome of fat grafting often leads to overcorrection or multiple operations [13].

Cell-assisted lipotransfer (CAL) based on ADSCs has become a promising cell therapy technology that can significantly increase the survival rate of fat grafts to 49.83–80.2% [5,14]. However, the existing obstacle for this method in clinical therapy is the unstable survival ratio of fat grafts and poor pathophysiological consequences (such as oily cysts and calcification) that still need to be improved [5]. Another CAL method also based on ADSCs is Stromal-vascular fractions (SVF) assisted fat grafted. SVF is a cell population containing ADSCs, fibroblasts and macrophages [3]. The disadvantage of SVF is that its cell population is complex and the proportion of its cell population cannot be standardized during the SVF isolation process, making the final fat retention rate still very uncertain [8,15]. In addition, it is worth mentioning that one study showed that fat grafting utilizing SVF rather than ADSCs as its CAL component had higher long-term retention rates, suggesting that other cells in SVF may contribute to fat retention rates improvement [16]. Based on this, we focused our research on fibroblasts that produce ECMs. Currently, the function of ECMs has been expanded to be considered a “niche” for stem cells [17,18]. Usually, all cells need to be adjacent to the ECMs to grow and reproduce [3]. Fibroblasts are the principal cell type that produces, maintains, and reabsorbs ECMs [19], but they also participate in the dynamic balance, remodeling of tissues, and the adjustment of interstitial fluid volume and pressure, thus realizing the steady state of tension, which could provide more space and growth opportunities for fat regeneration [20]. Additionally, adipose tissue rich in fibroblasts is more in line with the physiological structure of breast structural fat [21]. Moreover, fibroblasts not only provide a structural framework for all tissues but also serve as a repository for cytokines and growth factors and a scaffold for cell migration [22]. Importantly, fibroblasts have a strong ability to repair injuries that can differentiate into adipocytes, and they can also directly differentiate into hemangioendothelial cells to form new blood vessels [22]. Recently, fibroblasts have been used for wound healing and facial plastic surgery in the clinic [23].

In this study, we aimed to evaluate the function of fibroblasts on ADSCs in angiogenesis and lipogenesis and explore the underlying mechanisms based on proteomics in depth. Our data might provide helpful evidence to improve the survival and poor pathophysiological consequences of adipocytes in autologous fat grafting.

2. Materials and methods

2.1. Tissue cell separation, identification and culture

Normal adipose tissue and dermal tissue were obtained from 3 female patients with benign breast tumors between the ages of 30 and 70, and the distance between the obtained tissues and benign tumors was >5 cm [24]. A total of 15 ml of adipose tissue and $3 \times 3 \text{ mm}^3$ of skin tissue were obtained. ADSCs and fibroblasts were obtained from adipose and dermal tissue following previously published procedures, respectively [14]. Adipose tissue was digested in Dulbecco's modified Eagle's medium (DMEM, KeyGen BioTECH, China) with 0.1% (wt/vol) type II collagenase at 37 °C for 60 min. The dermal tissue was digested in DMEM with 0.1% (wt/vol) type I collagenase at 37 °C for 180 min. It was filtered through 70- μm cell strainers to remove any residual tissues, then centrifuged at $400 \times g$ for 5 min and washed twice, and the supernatant was discarded. The resulting cells were individually cultured until fully confluent.

ADSCs are identified in two ways. On the one hand, the amplified third-generation ADSCs were placed in a centrifuge tube (1×10^6 /tube), and the ADSCs were incubated with FIFC-conjugated monoclonal antibodies, specifically: CD73-FIFC (Cat#127219), CD90-FIFC

(Cat#328107), CD105-FIFC (Cat#323203), CD31-FIFC (Cat#303103), CD34-FIFC (Cat#343503) and CD45-FIFC (Cat#304005) with FIFC Human IgG1 (Cat#403507) as isotype control. All antibodies were from BioLegend. Cells were detached with 0.25% trypsin, washed in FACS buffer (1% fetal bovine serum, 0.1% NaN_3 in PBS), and mixed with directly conjugated monoclonal antibody (5 μl /100,000 cells) in FACS buffer incubate on ice for 30 min, wash twice with FACS buffer and fix with 1% paraformaldehyde/PBS. Detection was performed by flow cytometry and analysis was performed by Flowjo. On the other hand, ADSCs were identified by oil red O (OriCell, HUXMD-90031, American), alizarin red and alcian blue staining to identify adipose tissue, bone (OriCell, HUXMD-90021, American) and chondrocytes (OriCell, HUXMD-04041-2, American), respectively [25]. Fibroblasts are identified in two ways. On the one hand, cells were identified as fibroblasts by immunofluorescence with a monoclonal antibody against vimentin (vimentin, 1:500, rabbit, Abcam ab92547) [26]. On the other hand, fibroblasts were stained with CD10-FIFC (Cat#312207), CD26-FIFC (Cat#302704) and CD106-FIFC (Cat#A15439) monoclonal antibodies conjugated to APC, FIFC Human IgG1 (Cat#403507) was used as an isotype control [27,28]. All antibodies were from BioLegend except CD106-FIFC from Thermofisher. The method is the same as above for the identification of ADSCs. Human umbilical vein endothelial cells (HUVECs) were purchased from the Cell Bank of Shanghai Institutes for Biological Sciences (Shanghai, China). HUVECs and fibroblasts were cultured in DMEM supplemented with 10% fetal bovine serum (FBS; Gibco) and 1% penicillin/streptomycin (Gibco). ADSCs were cultured in Preadipocyte Medium (PAM, ScienCell, USA).

Human umbilical vein endothelial cells (HUVECs) were purchased from the Cell Bank of Shanghai Institutes for Biological Sciences (Shanghai, China). HUVECs and fibroblasts were cultured in DMEM supplemented with 10% fetal bovine serum (FBS; Gibco) and 1% penicillin/streptomycin (Gibco). ADSCs were cultured in Preadipocyte Medium (PAM, ScienCell, USA).

2.2. Adipogenicity of ADSCs and fibroblasts

To evaluate the reciprocal effect between ADSCs and fibroblasts on adipogenic differentiation ability, we conducted an induced differentiation assay in a co-culture system. For the Transwell co-culture model, ADSCs at a density of 2×10^5 cells/well were seeded in the lower chamber of a 6-well plate, and fibroblasts with a 0.4-microm pore size (3412; Corning) were placed on the top of each well followed by seeding with 2×10^4 cells/well in the upper chamber of the Transwell as the experimental group [29]. A separate culture group of ADSCs and fibroblasts was used as a control. After that, the medium was changed to a Human Adipose Mesenchymal Stem Cell Adipogenic Differentiation Kit (HUXMD-04041-2, OriCell). Two weeks later, oil red O staining was used to detect lipid formation [30,31].

2.3. Hemangioendothelial differentiation of ADSCs and fibroblasts

To evaluate the reciprocal effect between ADSCs and fibroblasts on the hemangioendothelial cell differentiation capability, we conducted an induced differentiation assay in a co-culture system. Groups and plated cells were divided in the same way as described above. When the cells reached 70–90% confluency, the medium was replaced with endothelial medium (DMEM + 30% human serum (From the patients, the collection method is as described [32], 50 ng/ml VEGF [Sigma–Aldrich, USA], 10 ng/ml bFGF [Sigma–Aldrich, USA]) for 7 days. The medium was changed every 2 days. Anti-Factor VIII (Abcam, USA) was used to identify differentiated hemangioendothelial cells by immunofluorescence staining.

2.4. Co-culture of cells under ischemia and hypoxia

To mimic hypoxic conditions immediately after fat grafting, we performed a Transwell co-culture model under 5% O₂. We divided the cells into three groups: an ADSC and fibroblast co-cultured group and ADSC and fibroblast groups cultured separately. Briefly, after cells attached to the culture dish, the original complete culture medium was replaced with 10 ml serum-free PAM and placed in an anoxic incubator. Hypoxia was induced by using a multifunctional incubator (Thermo, USA), and the O₂ concentration was maintained at 5% with a mixture composed of CO₂ and balanced N₂ for 72 h [33]. After 72 h, we collected the supernatant from each sample and centrifuged it at 3000g for 10 min before discarding the pellet and subjecting the supernatant to subsequent experiments [34].

2.5. Cell Counting Kit 8 analysis

Cells were seeded at 2×10^3 cells/well in 96-well plates and incubated for 48 h at 37 °C with 5% CO₂. Cells were incubated with 10 µl CCK8 labeling reagent (0.5 mg/ml; Dojindo, Japan) and 100 µl serum-free medium per well for 2 h. At three time points of 0 h, 24 h, and 48 h, the cell viability was calculated by using a microplate reader (Thermo Scientific, Shanghai, China) to detect the absorption at 450 nm [35].

2.6. Cell migration

Wound healing and Transwell studies were used to determine the migration rate of HUVECs. Three lines at 1 cm intervals were painted behind 6-well plates in the wound healing assay. HUVECs were seeded into 6-well plates at a density of 6×10^5 cells/well with different supernatant treatments as described above, and the cells were scratched with lines perpendicular to the previously painted line. Three fields were randomly selected from each well, and cell movements in the scratch were observed and photographed at 0 h, 24 h, and 48 h. The width of the scratch was detected with ImageJ 1.8 software. Meanwhile, a Transwell filter assay (Minicell, Millipore, USA) was used to quantify cell invasion. HUVECs were added to the upper chamber with 8.0-µm pore size membrane inserts in 24-well plates at a density of 5×10^3 . Cells that migrated to the outside of the membrane were stained with crystal violet (Beyotime) after 24 h. The cells were counted at 100× magnification in five randomly selected regions per well, and all these experiments were repeated at least three times [35].

2.7. Flow cytometry

ADSCs were co-cultured with or without fibroblasts separately under hypoxic conditions. These cells were harvested and centrifuged at 1300 rpm for 5 min at 72 h, and the cells pellet was washed with ice-cold D-Hanks (pH 7.2–7.4). The cells pellet was suspended in 200 µl of 1× binding buffer, and 10 µl Annexin V-APC was added to stain cells in the dark for 15 min. Apoptotic cells were detected by flow cytometry and analyzed by FlowJo [36].

2.8. Endothelial tube formation assay

Ischemia and hypoxia model cells, as well as supernatant collection, are depicted above. HUVECs were cultured with ADSCs and fibroblast co-culture supernatant as the experimental group. HUVECs were cultured with ADSC and fibroblast supernatant separately, with HUVECs serum-free culture serving as a control group. HUVECs were seeded onto 96-well plate-coated matrix gels (BD Biosciences) and treated separately with the three lysates in 5% CO₂ at 37 °C for 12 h. The resulting tubular structures were imaged

using a light microscope, and the total number of connections was automatically calculated using the Angiogenesis Analyzer plug-in in ImageJ 1.8 software [37].

2.9. Quantitative polymerase chain reaction (qPCR)

We performed qPCR experiments on ADSCs co-cultured with fibroblasts, and ADSCs cultured alone (Cell culture conditions are shown in the co-culture of cells under ischemia and hypoxia section). Total RNA was extracted using a High Pure RNA Isolation kit (Roche). cDNA was obtained by reverse transcription-PCR from 1 µg of RNA using SuperScript VILO cDNA synthesis (Invitrogen) according to the manufacturer's instructions. Gene expression was analyzed by real-time qPCR using LightCycler 480 SYBR green I master mix (Roche), corrected by GAPDH expression and expressed as relative units. The primer sequences used for qPCR are listed in [Supplementary Table 1](#).

2.10. Construction of a fat-grafted BALB/c nude mouse model

Animal experiments were approved by the Institutional Animal Care and Use Committee of Nanjing Medical University (Nanjing, China). Female BALB/c nude mice (3–4 weeks old) were purchased from the University Model Animal Research Center of Nanjing Medical University and raised under SPF conditions in the animal room of Nanjing Medical University.

As described above, after obtaining primary ADSCs and fibroblasts, these two cell lines were expanded in vitro to obtain the cells required for subsequent experiments. After grinding the adipose tissue into a chyle, it was centrifuged at 1200×g for 3 min to obtain the purified fat required for this experiment, that is, the “Coleman fat” in the middle layer [38] (Fig. 4A and B).

Fibroblasts and ADSCs were counted for cell viability using a Countess® II automated cell counter prior to autologous fat grafting (Fig. 4C). Twenty BALB/c nude mice were divided into 4 groups with 5 mice in each group. The cell density of all CAL groups was 2×10^7 /ml. The first group was fibroblasts combined with ADSCs (the ratio of cells was fibroblasts vs ADSCs, 1:5) mixed with fat; the second group was fibroblasts mixed with fat; the third group was ADSCs mixed with fat; the fourth was fat grafted. Finally, the left side of the second pair of mammary fat pads of BALB/c nude mice was injected with grafted fat or fat with mixed cells, and the injection volume of each group was 200 µL. The volume calculation formula was total volume (mm³) = length × width²/2 [39]. At 12 weeks posttransplant, following imaging studies, fat specimens were removed, weighed, and fixed in 4% paraformaldehyde for further analysis.

2.11. CT and 3D reconstruction

At week 12 after fat grafting, microcomputed tomography (microCT) and imaging were performed using a Bruker Skyscan 1276 microCT (Bruker) to measure the volume of grafted fat in BALB/c nude mice. 3D reconstruction was performed using cubic spline interpolation, and the mean value was calculated for each sample. The assessment of graft fat volume was performed by two investigators in a single-blind setting [40].

2.12. Ultrasonography

We performed ultrasound examinations using a MyLab™Delta ultrasound system (SL3116, Esaote, Genoa, Italy). We exposed anesthetized BALB/c nude mice to 20 MHz, pulsed USW, and a scan rate of 35 frames per second for 2–3 min. The grafted fat of BALB/c

nude mice was scanned to evaluate the occurrence of oily cysts in BALB/c nude mice in each group [41].

2.13. Histological staining

At the observation end point at week 12, after the above-mentioned examinations were completed, the grafted fat removed from the subcutaneous tissue was fixed in 4% paraformaldehyde for 12 h, embedded in paraffin, and sectioned (8 μm thickness). Masson's staining (acid fuchsin staining for 5–10 min, aniline blue staining for 5 min) was used to analyze the distribution of surviving adipocytes and their surrounding ECMs. Three randomly selected regions in each sample (sample size per group, n = 3) were imaged under an inverted microscope (Olympus Corporation) [42].

For immunofluorescence histology staining, tissue sections were probed with primary antibodies overnight at 4 °C and then incubated with CyTM3-conjugated secondary antibodies or Alexa Fluor 488-conjugated secondary antibodies. The following primary antibodies were used for immunohistochemistry: F4/80 (D4C8V) XP[®] Rabbit mAb, anti-Human Nuclear Antigen, anti-Perilipin, and anti-CD34. Staining was performed according to the reagent manufacturer's instructions. A microscope was used to take photomicrographs. Among them, type 2 macrophages were labeled with F4/80, and the fluorescent color was green; the anti-Perilipin antibody labeled adipocytes, and the fluorescent color was orange; the anti-CD34 antibody labeled hemangioendothelial cells, and the fluorescent color was red. Five randomly selected regions in each sample (sample size per group, n = 3 per group) were imaged [43].

2.14. Statistics

Data were visualized, and statistical analyses were performed using Prism 8.0 software (Graph Pad) or the R statistical package. $P < 0.05$ was considered statistically significant. In all cases, the experimental groups showed comparable variance. Each experiment was performed in triplicate. P values for unpaired comparisons between two groups with comparable variance were calculated by two-tailed Student's t test. * $P < 0.05$, ** $P < 0.01$, *** $P < 0.001$, **** $P < 0.0001$. Error bars indicate the mean ± s.d., as indicated.

3. Results

3.1. Fibroblasts regulate the proliferation, apoptosis, and adipogenic and hemangioendothelial cells differentiation of ADSCs

Primary fibroblasts and ADSCs were successfully isolated from human tissues and identified separately. ADSCs were identified by CD73+, CD90+, CD105+, CD31-, CD34- and CD45- [44,45], and by their ability to differentiate into adipogenic, chondrogenic and osteogenic (Supplementary Fig. 1). Fibroblasts are not fully capable of adipogenic, chondrogenic and osteogenic differentiation [28,46]. Fibroblasts were identified by CD10+, CD26+, CD106- [27,28] and immunofluorescence chemical staining of vincentin (Supplementary Fig. 2).

ADSCs apoptosis was inhibited by fibroblasts (Fig. 1A). Fibroblasts promoted the proliferation of ADSCs whether they are co-

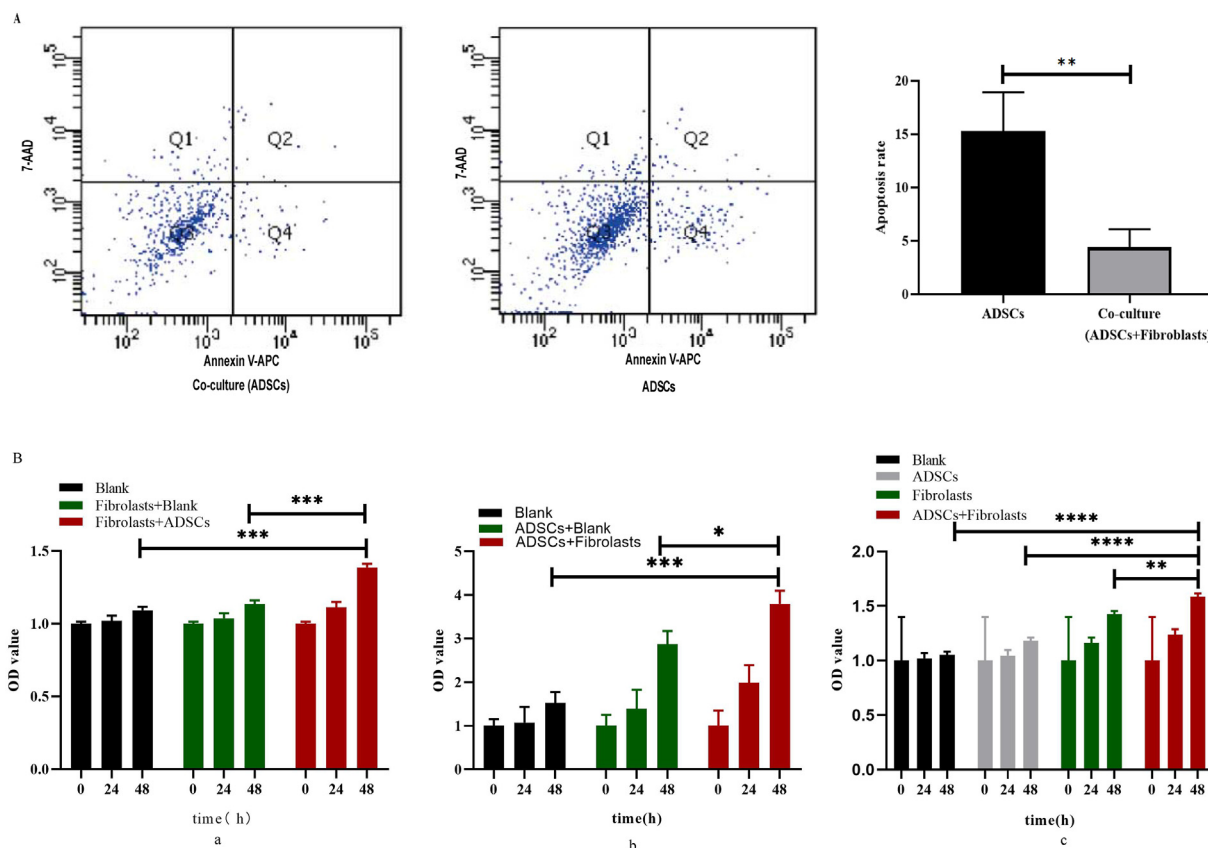


Fig. 1. Effects of ADSCs and fibroblasts on the proliferation and apoptosis of each other. A: Representative scatter plots of flow cytometry analysis to measure apoptosis by staining ADSCs with Annexin V-APC and 7-AAD. The apoptosis rate of ADSCs in ADSCs co-cultured with fibroblasts was lower than that in ADSCs cultured alone. B: ADSCs and fibroblasts promote each other's proliferation. a: ADSCs promote the proliferation ability of fibroblasts. b: Fibroblasts promote the proliferation ability of ADSCs. c: The proliferation ability of fibroblasts and ADSCs when co-cultured is greater than their respective proliferation abilities when they are cultured separately. Student's t test was used to analyze the data, and the asterisks represent significant differences between the groups (* $P < 0.05$, ** $P < 0.01$, *** $P < 0.001$, **** $P < 0.0001$, n = 3).

cultured in indirect contact co-culture (Fig. 1B-b) or direct contact (Fig. 1B-c). The results showed a beneficial interaction between the two kinds of cells. In the adipogenic differentiation experiment, the co-culture of fibroblasts and ADSCs was performed as the experimental group, and fibroblasts and ADSCs were cultured separately as two control groups. The results demonstrated that the adipogenic (Fig. 2A, co-culture [ADSCs] > ADSCs, $P < 0.05$) and hemangioendothelial cells (Fig. 2B, co-culture [ADSCs] > ADSCs, $P < 0.05$) differentiation capacities of ADSCs were improved by fibroblasts in the co-culture group.

3.2. ADSCs regulate the proliferation, adipogenic and hemangioendothelial cells differentiation of fibroblasts

We found that ADSCs promoted not only the proliferation of fibroblasts (Fig. 1B-a) but also the differentiation of adipocytes (Fig. 2A, co-culture [Fibroblasts] > Fibroblasts, $P < 0.05$) and hemangioendothelial cells (Fig. 2A, co-culture [Fibroblasts] > Fibroblasts, $P < 0.05$). However, unlike fibroblasts, which could inhibit the apoptosis of ADSCs, ADSCs could not inhibit fibroblast apoptosis (Negative results not shown). The results also showed that the adipogenic (Fig. 2A) and hemangioendothelial cells (Fig. 2B) differentiation capacities of ADSCs were better than those of fibroblasts, whether in co-culture or separate cultures.

3.3. Co-culture system promotes angiogenesis, proliferation, and migration capabilities of HUVECs

Compared with the fibroblast or ADSC supernatant, the co-culture supernatant significantly promoted angiogenesis (Fig. 3A), proliferation (Fig. 3C), and migration (Fig. 3B, D) of HUVECs, indicating that the secretory components of the co-culture supernatant play important roles in the proliferation, angiogenesis and migration processes of HUVECs.

3.4. Changes in angiogenesis and adipogenic factors expression in the co-culture group

In the process of exploring the mechanism of this part of the experiment, we detected the expression of classical angiogenesis and adipogenesis factors (PPAR γ , bFGF, VEGF, C/EBP α , C/EBP β , FABP4, Leptin, Adiponectin, IGF1, GAPDH [16,47,49]). We found that only VEGF, C/EBP α and IGF1 were significantly increased in the co-culture group of ADSCs and fibroblasts compared to ADSCs cultured alone (Supplementary Fig. 3).

3.5. Process and volume analysis of fat grafting

Before performing CAL fat grafting experiments, we successfully isolated and expanded fibroblasts and ADSCs from human tissues

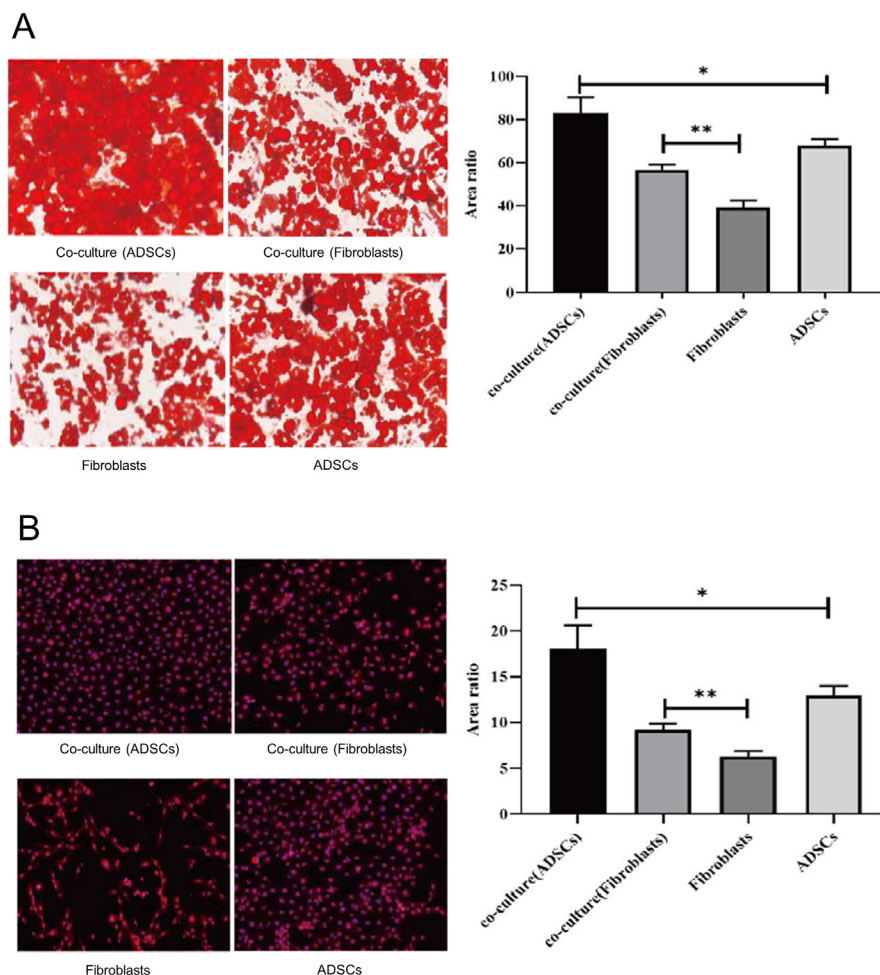


Fig. 2. Adipogenic and hemangioendothelial cells differentiation of ADSCs and fibroblasts. A: The capacity of ADSCs and fibroblasts to differentiate into adipocytes was improved when they were co-cultured. B: The capacity of ADSCs and fibroblasts to differentiate into hemangioendothelial cells was improved when they were co-cultured (* $P < 0.05$, ** $P < 0.01$, *** $P < 0.001$, **** $P < 0.0001$, $n = 3$).

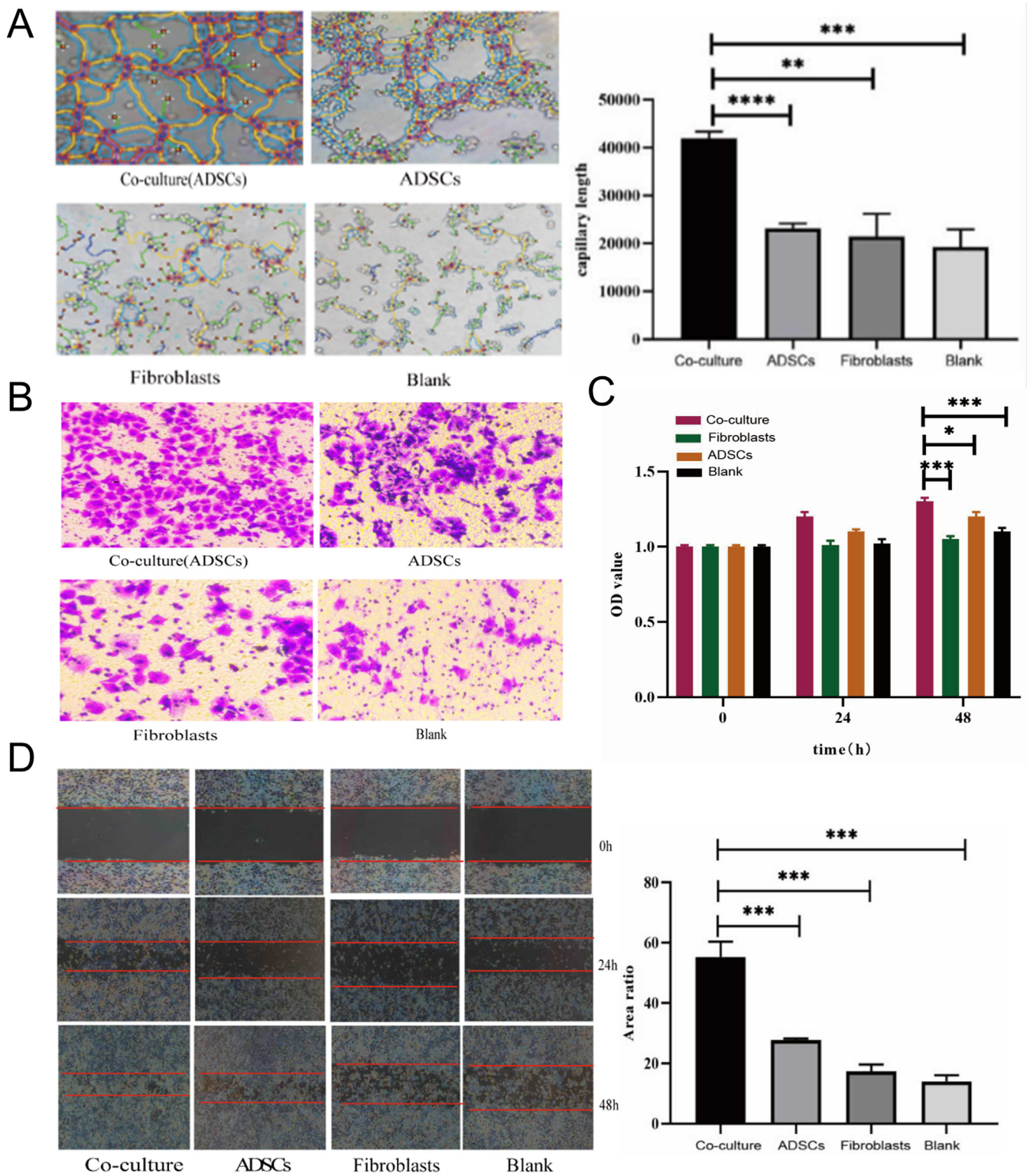


Fig. 3. A Co-culture system of ADSCs combined with fibroblasts promotes angiogenesis, proliferation, and migration capabilities of HUVECs. A: Co-culture supernatant of ADSCs combined with fibroblasts can considerably improve the angiogenesis of HUVECs when compared to fibroblast or ADSCs supernatant. B: In the Transwell filter assay, compared with fibroblasts or ADSCs supernatant, the co-culture supernatant of ADSCs combined with fibroblasts significantly promoted the migration of HUVECs. C: Co-culture supernatant of ADSCs combined with fibroblasts can considerably promote the proliferation of HUVECs when compared to fibroblast or ADSCs supernatant. D: In the wound healing assay, compared with the fibroblasts or ADSCs supernatant, the co-culture supernatant of ADSCs combined with fibroblasts significantly promoted the migration of HUVECs (* $P < 0.05$, ** $P < 0.01$, *** $P < 0.001$, **** $P < 0.0001$, $n = 5$).

in vitro (Fig. 4A), and purified fat was obtained using the “Coleman” method [38] (Fig. 4B). When fat grafting was performed, we determined the viability of viable cells. The viable viability of fibroblasts and ADSCs were 89% and 94%, respectively (Fig. 4C). The construction of a complete fat graft model is shown in Fig. 4. In preliminary experiments, we found that the fibroblasts combined with ADSCs (cell ratio of 1:5, the following are the former than the latter) mixed with fat group, could most effectively maintain the volume of grafted fat. Therefore, in the follow-up study, we selected the group of fibroblasts combined with ADSCs (cell ratio of 1:5) as a representative group of fibroblasts combined with ADSCs for fat grafting.

We found that after fat grafting, from week 8 to week 12, the fibroblasts combined with ADSCs mixed with fat group had a significantly higher rate of regeneration of the grafted fat volume than the other three groups. At the 12th week after fat grafting, the volume of grafted fat was measured by micro-CT tomography + 3D reconstruction. In all four groups, the volume of grafted fat was ranked from high to low (Fig. 5B): the fibroblasts combined with ADSCs mixed with fat group ($190 \text{ mm}^3 \pm 4\%$), the ADSCs mixed with fat group ($135 \text{ mm}^3 \pm 3.2\%$), the fibroblasts mixed with fat group ($103 \text{ mm}^3 \pm 4.8\%$), and the fat group ($25 \text{ mm}^3 \pm 5\%$).

3.6. Qualitative analysis of fat grafts

The ultrasound results (Fig. 6A) showed that compared with the three groups of ADSCs combined with fat, fibroblasts combined with fat, and fat, the formation of oily cysts in the fibroblast combined with ADSCs mixed with fat group was much less than the levels in the other three groups. Tissue integrity and grafted fat volume were much higher than those of the other three groups.

The results of Masson’s staining showed that the combination of fibroblasts combined with ADSCs in the mixed adipose group had the best morphology, rich ECMs (Fig. 6B), and maintained the normal adipose tissue structure, which may be due to the ECMs

secreted by fibroblasts supporting the adipose tissue. The space for the cells so that they do not pile up excessively due to reduced oxygen consumption.

As seen from the results of immunofluorescence staining (Fig. 7), in the fibroblasts combined with ADSCs mixed adipocyte group, a large number of viable and morphologically healthy adipocytes (perilipin [orange fluorescence] was strongly positive) could be seen, and fat-abundant hemangioendothelial cells (CD34 [red fluorescence]) were present around the cells. In the fibroblast-mixed adipose group and the ADSCs-mixed adipose group, there were fewer viable adipocytes, and microscopic oily cysts surrounded by macrophages (F4/80 (highly positive for [green fluorescence])) appeared. This phenomenon was found to be even more pronounced in simple fat grafts, where large oily cysts encased in large numbers of macrophages were present, and a large number of adipocytes did not survive or regenerate.

4. Discussion

After avascular fat grafting, severe ischemia and hypoxia promote adipocyte necrosis and apoptosis. In contrast, ADSCs can survive under extreme conditions of ischemia and hypoxia for three days and promote tissue regeneration [50]. However, CAL based on ADSCs has an insufficient survival rate and severe adverse reactions in autologous fat grafting. We discovered that adding fibroblasts to ADSCs improves adipogenic and angiogenic differentiation, proliferation, and anti-apoptotic properties, which could be a new strategy to improve CAL survival and adverse effects.

Fibroblasts and ADSCs promoted the proliferation of each other, and fibroblasts inhibited ADSC apoptosis. The effects of ADSCs on the biological functions of fibroblasts and the secretion of ECMs through secretion have been studied and confirmed [51]. Fibroblasts and ADSCs have the ability to differentiate into adipocytes and hemangioendothelial cells and support their growth [52–56]. Our study demonstrated that when ADSCs were co-cultured with

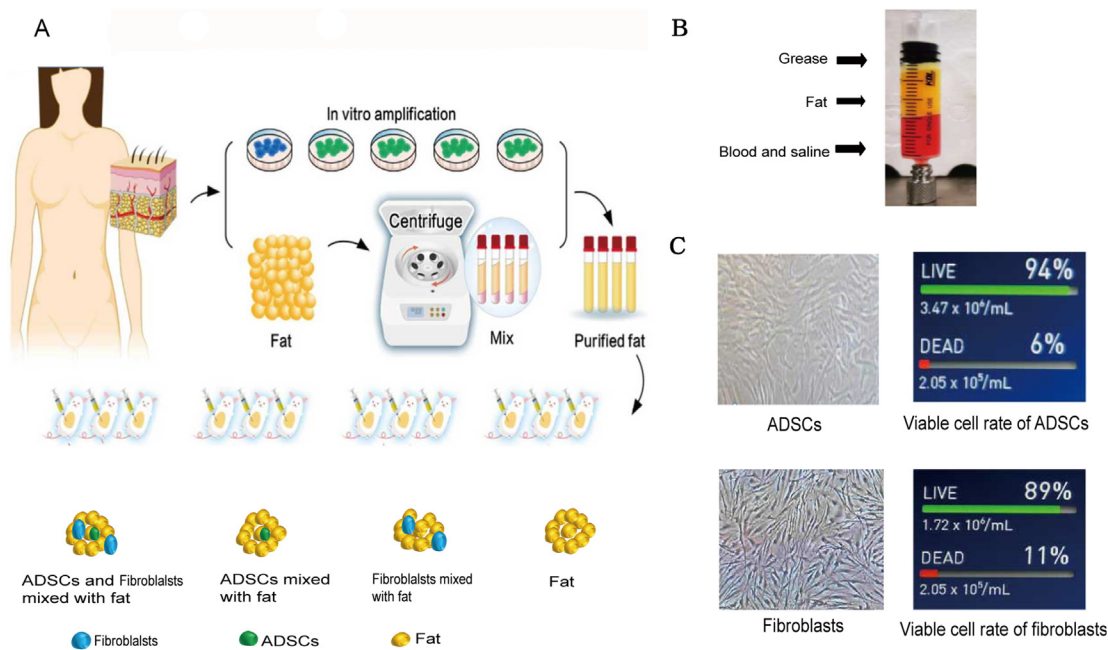


Fig. 4. Process of fat grafting. A: Fibroblasts, ADSCs (and expanded in vitro) and adipose tissue (purified) were isolated from human tissues and divided into the following groups: fibroblasts combined with ADSCs mixed with adipose group, ADSCs mixed with adipose group, fibroblasts mixed with adipose group, and fat group. The four groups were subcutaneously grafted into BALB/c nude mice. B: The purified adipose tissue is divided into three layers: the top layer is the oil layer, the middle layer is the purified fat layer, and the bottom layer is the blood and normal saline. C: Determination of ADSCs (94% viability) and fibroblast viability (89% viability) before fat grafting.

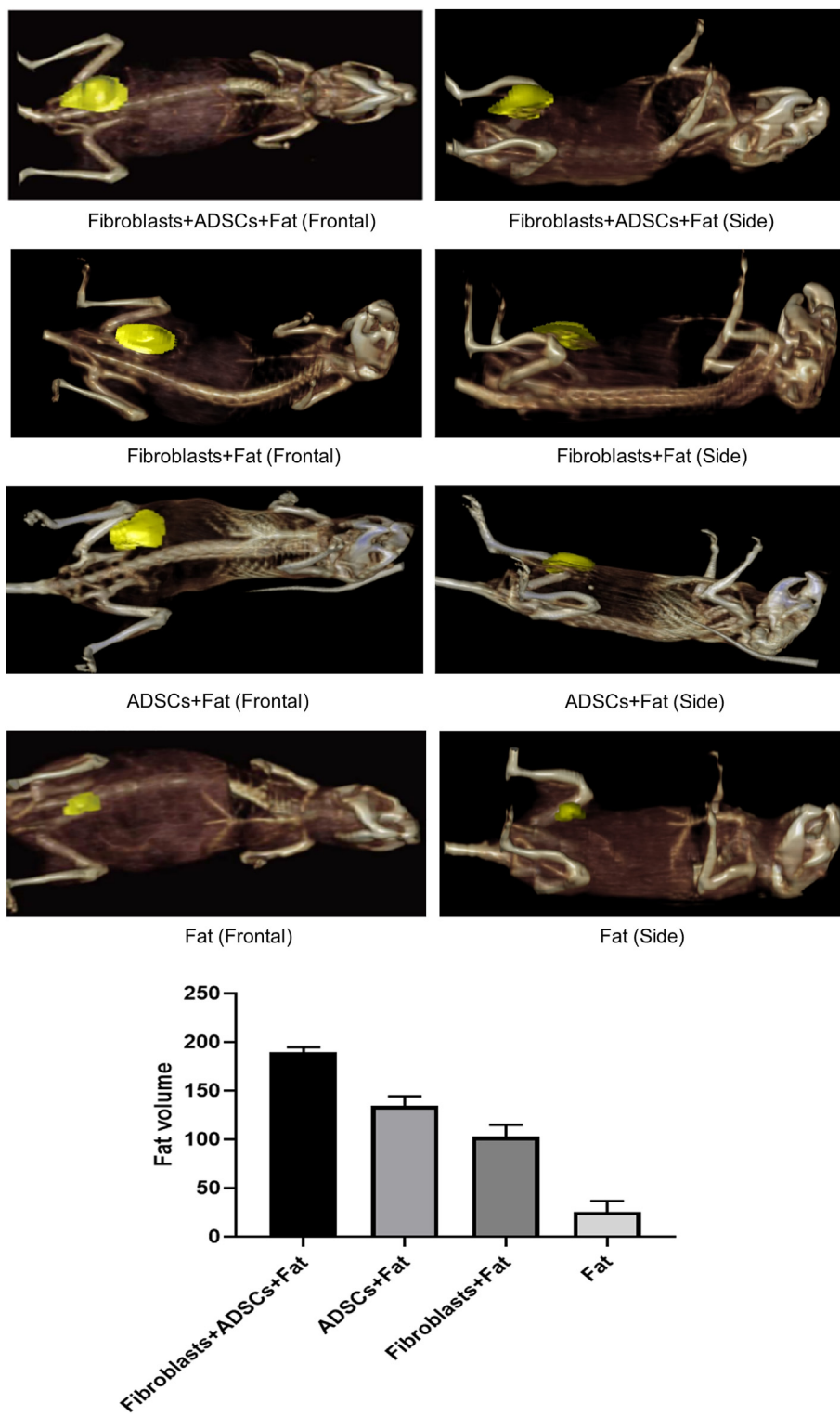


Fig. 5. Micro-CT + 3D reconstruction for assessment of grafted fat volume. At the 12th week after fat grafting, micro-CT + 3D reconstruction was used to measure the fibroblasts combined with ADSCs mixed with fat group, the ADSCs mixed with purified fat group, the fibroblasts mixed with purified fat group, and the fat group with transplanted fat volume. (n = 5).

fibroblasts, adipogenic differentiation and hemangioendothelial cells were enhanced compared to when the two types of cells were cultured separately. A previous study showed that fibroblasts are the preferred source of cells to promote blood vessel formation when co-cultured with HUVECs [56], and ADSCs can promote the

migration and invasion abilities of HUVECs [56]. ADSCs also promote the proliferation and migration of fibroblasts [57]. The purpose of our study was to determine whether ADSCs combined with fibroblasts and HUVECs have any effect on HUVECs when they are co-cultured together. We found that the collection of fibroblasts

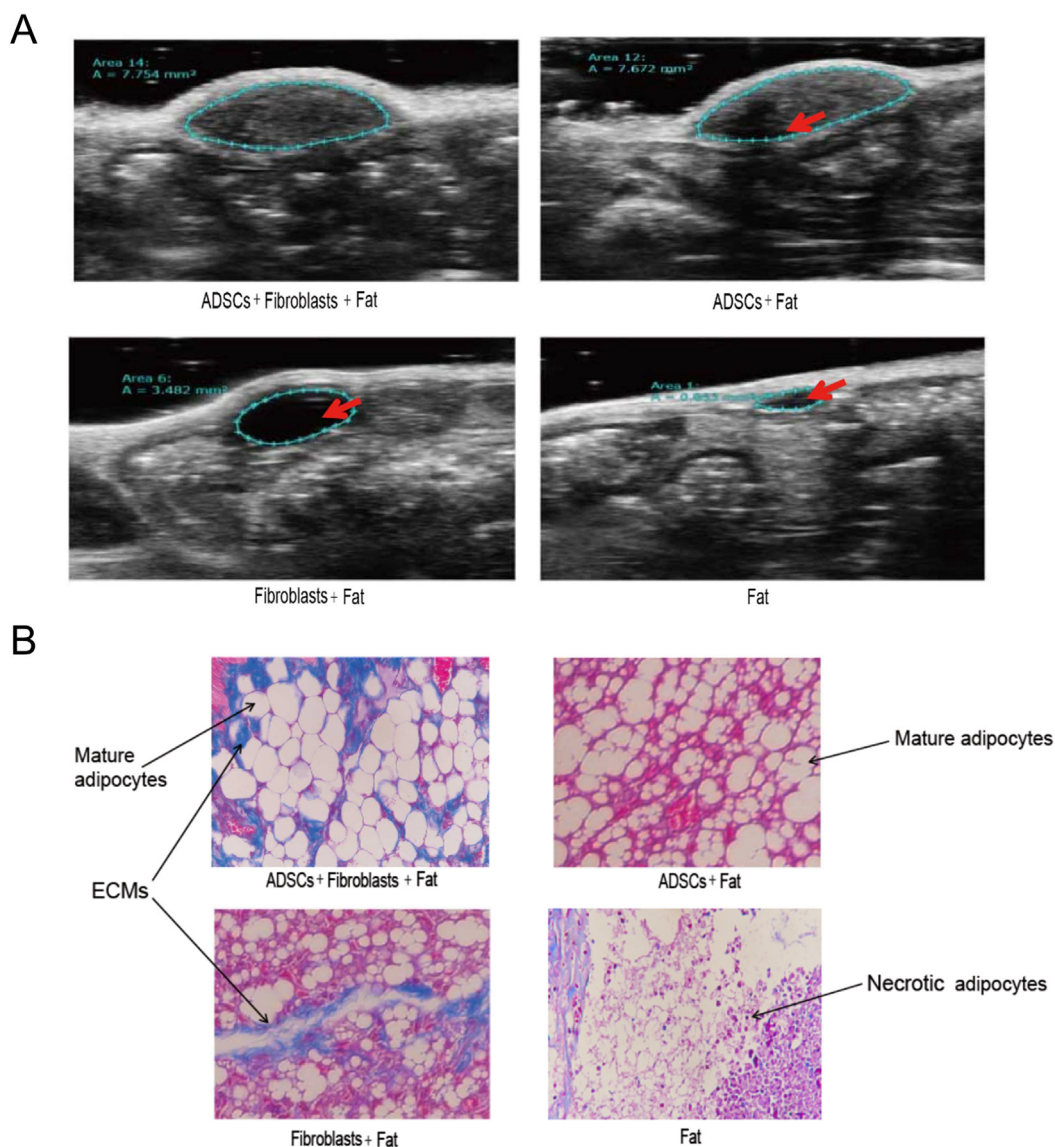


Fig. 6. A: Ultrasound showing the occurrence of oily cysts (red arrows) at 12 weeks after fat grafting. B: Masson's staining. (n = 5).

and ADSCs under hypoxic conditions under the co-culture supernatant and secreted substances promoted angiogenesis, proliferation, and the migration of HUVECs. Hence, it is necessary to clarify which substances secreted between cells caused the above results.

We detected by qPCR that in ADSCs co-cultured with fibroblasts, vascular endothelial growth factor VEGF, adipogenic differentiation factor *C/EBP α* and IGF1 (*C/EBP α* -induced adipocyte production [58,59], IGF1 promotes adipogenesis through ADSCs [60]) mRNA expression levels were elevated compared with those in ADSCs cultured alone.

In *in vivo* experiments, we isolated and expanded ADSCs and fibroblasts from human tissues and obtained purified fat. The experiment was divided into a preexperiment and a formal experiment. Three BALB/c nude mice were set up in each group, and the cell density was 2×10^7 /ml (in the previous clinical study of CAL, when the density of ADSCs was 2×10^7 /ml, that is, 2000 times the physiological level, the fat retention rate was the highest, and this ratio was used as the lower limit. When this density is exceeded, the fat retention rate will not be affected [5,61]). The fat grafted site was the second pair of mammary fat pads of BALB/c nude mice.

In our preliminary experiments, we found that a 1:5 ratio of fibroblasts + ADSCs was most favorable for the volume retention of grafted fat, so this ratio was adopted in subsequent experiments. We found that the fibroblasts combined with ADSCs mixed with fat group had the highest volume retention rate ($190 \text{ mm}^3 \pm 4\%$), the lowest occurrence of oily cysts, the best fat morphology, and the most uniform distribution of the ECMs.

From our *in vitro* experiments, it can be seen that in the co-culture system of fibroblasts and ADSCs, the adipogenic differentiation abilities of fibroblasts and ADSCs were enhanced, the angiogenesis, proliferation and migration abilities of HUVECs were promoted, and fibroblasts and ADSCs also promoted each other's proliferation. In addition, fibroblasts had anti-apoptotic effects of ADSCs.

These *in vitro* experiments explain why, in animal experiments, when fibroblasts were combined with ADSCs mixed with fat, the grafted fat had the highest rate of fat volume retention or regeneration and the lowest occurrence of the adverse effect of oily cysts. In addition to the improved survival rate of grafted cells, the reason for the lowest occurrence of oily cysts is that the ECMs secreted by

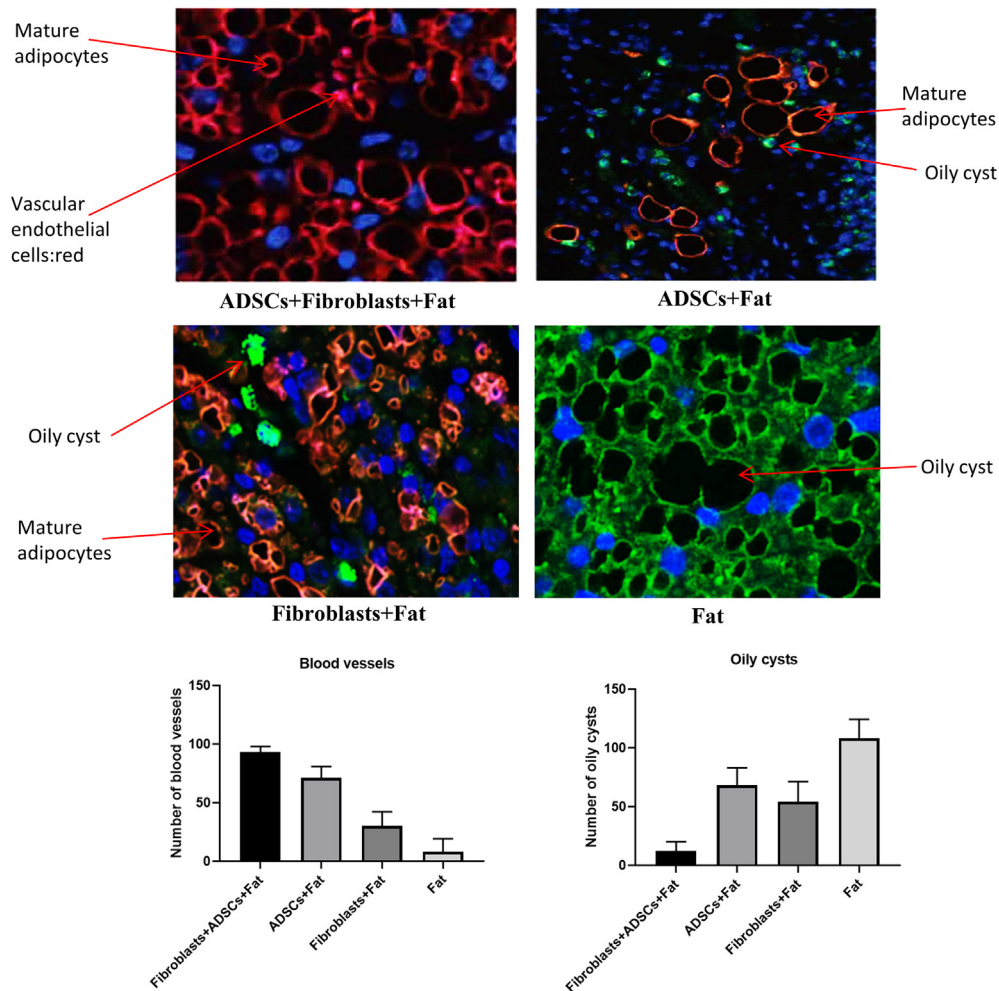


Fig. 7. Immunofluorescence staining. Immunofluorescent staining of adipocytes with perilipin (orange), macrophages with F4/80 (green), and hemangioendothelial cells (red) in 4 different subgroups at week 12 after fat grafting. Abundant hemangioendothelial cells can be seen in adipocyte-rich areas, and oil droplets or dead adipocytes are encapsulated by macrophages to form oily cysts. (n = 5).

fibroblasts were distributed and interspersed among the relatively large fat cells, which could give rise to ADSCs having more space and targeted differentiation opportunities.

Our research clarified the following issues. 1. We first discovered that the co-culture of ADSCs and fibroblasts could be an effective way to improve the survival rate of autologous fat grafting. 2. In the current study, the most common complication of autologous fat-grafted oily cysts [5,61] is usually a lack of discussion and accurate evaluation (ultrasound examination of oily cysts is the most objective and accurate) [62]. Our research addresses and preliminarily solves this defect. 3. Compared with CAL or traditional autologous fat grafting, introducing fibroblasts is more in line with the physiological structure of breast structural fat and improves the spatial organization [21]. 4. In our study, fibroblasts mixed with fat also significantly increased the rate of fat retention or regeneration [52–55]. In CAL, other studies have not reported this finding. At present, it seems that the use of fibroblasts alone to assist autologous fat grafting is not the optimal autologous grafting scheme, but in certain cases, the use of fibroblasts as CAL can also be considered an option.

Furthermore, ADSCs and fibroblasts can be cryopreserved and applied in the future. ADSCs can reconstruct and repair target organs (e.g., bone, cartilage, myocardium, liver, nervous system, and skin) [63]. ADSCs can also treat lymph node edema after breast

cancer surgery [64] and reverse tissue damage, such as damage that occurs during radiotherapy [65,66]. 2. Fibroblast grafting includes the treatment of gingival recession [67,68], nonhealing wounds [69], diabetic foot ulcers [70], wrinkles [42], acne scars [71], and moderate to severe nasolabial folds [72]. Fibroblasts can also replace the role of the skin flap. Currently, FDA-approved Derma-graft® is a sterile, cryopreserved human fibroblast-derived dermal substitute [23]. In breast reconstruction, this fibroblast-based material can be used clinically in place of skin flaps, eliminating the need to remove large areas of skin from the human body.

The safety of CAL is widely recognized in clinical practice. Since the first grafting of adult stem cells from bone marrow in the 1960s [71] and the grafting of adult stem cells from cord blood in 1988, there has been no scientific literature on any record of tumor formation caused by the injection of stem cells [67,73].

There are several limitations of our study. First, we require additional human research to verify our findings. Then, no molecular mechanism has been discovered to explain how co-cultured fibroblasts and ADSCs govern cell differentiation, proliferation, migration, anti-apoptosis, and other characteristics by signaling pathways and target molecules. Finally, the clinical application of CAL has some limitations. The processing time for expanded cells is also longer and more expensive in CAL compared to traditional fat grafting. Therefore, after the cells are harvested, the production of

low-cost, minimally manipulated expanded cells that can be safely used in the operating room is a major challenge in applying our method to the field of regenerative medicine. It is not an easy task to expand cells *in vitro* and then infuse or transplant them back into the human body. Fibroblast + ADSCs assisted fat graft still needs considerable research before it becomes a standard clinical application.

5. Conclusion

Our experiments indicate that the co-culture of ADSCs and fibroblasts could help improve the application prospects of CAL in reconstruction and cosmetic volume restoration, making this method the most attractive option in the field of autologous fat grafting.

Statement of human and animal rights, or ethical approval

The animal research in this paper has been ethically approved by our hospital (IACUC-2011050).

Informed consent

For this type of study informed consent is not required.

Availability of data and materials

All data and materials used in this work were publicly available and also available based on request.

Author contributions

KL, SSD and HTF were responsible for the integrity of the entire study and study design. HTF drafted the manuscript initially. HTF, SSD and KL performed the analyses. HTF prepared the figures and tables for the manuscript. All authors read and approved the final manuscript.

Funding

There was no funding source for this study.

Declaration of competing interest

The authors declare that they have no known competing financial interests or personal relationships that could have appeared to influence the work reported in this paper.

Acknowledgments

No additional acknowledgments.

Appendix A. Supplementary data

Supplementary data to this article can be found online at <https://doi.org/10.1016/j.reth.2022.11.008>.

References

- [1] Ward ZJ, Atun R, Hricak H, Asante K, McGinty G, Sutton EJ, et al. The impact of scaling up access to treatment and imaging modalities on global disparities in breast cancer survival: a simulation-based analysis. *Lancet Oncol* 2021;22(9):1301–11.
- [2] Krastev T, Van Turnhout A, Vriens E, Smits L, van der Hulst R. Long-term follow-up of autologous fat transfer vs conventional breast reconstruction and association with cancer relapse in patients with breast cancer. *JAMA Surg* 2019;154(1):56–63.
- [3] Tracy LE, Minasian RA, Cateson EJ. Extracellular matrix and dermal fibroblast function in the healing wound. *Adv Wound Care (New Rochelle)* 2016;5(3):119–36.
- [4] Blondeel PN, Hijjawi J, Depypere H, Roche N, Van Landuyt K. Shaping the breast in aesthetic and reconstructive breast surgery: an easy three-step principle. *Plast Reconstr Surg* 2009;123(2):455–62.
- [5] Kolle ST, Duscher D, Taudorf M, Fischer-Nielsen A, Svalgaard JD, Munthe-Fog L, et al. Ex vivo-expanded autologous adipose tissue-derived stromal cells ensure enhanced fat graft retention in breast augmentation: a randomized controlled clinical trial. *Stem Cells Transl Med* 2020;9(11):1277–86.
- [6] Doloff JC, Veisoh O, De Mezerville R, Sforza M, Perry TA, Haupt J, et al. The surface topography of silicone breast implants mediates the foreign body response in mice, rabbits and humans. *Nat Biomed Eng* 2021;5(10):1115–30.
- [7] Decoster RC, Lynch EB, Bonaroti AR, Webster JM, Butterfield TA, Evers BM, et al. Breast implant-associated anaplastic large cell lymphoma: an evidence-based systematic review. *Ann Surg* 2021;273(3):449–58.
- [8] Cai W, Yu LD, Tang X, Shen G. The stromal vascular fraction improves maintenance of the fat graft volume: a systematic review. *Ann Plast Surg* 2018;81(3):367–71.
- [9] Schopf SSJ, Hommes JE, Krastev TK, Derks D, Larsen M, Rakhorst H, et al. BREAST trial study protocol: evaluation of a non-invasive technique for breast reconstruction in a multicentre, randomised controlled trial. *BMJ Open* 2021;11(9):e051413.
- [10] Gill PS, Hunt JP, Guerra AB, Dellacroce FJ, Sullivan SK, Boraski J, et al. A 10-year retrospective review of 758 DIEP flaps for breast reconstruction. *Plast Reconstr Surg* 2004;113(4):1153–60.
- [11] Hofer SO, Damen TH, Mureau MA, Rakhorst HA, Roche NA. A critical review of perioperative complications in 175 free deep inferior epigastric perforator flap breast reconstructions. *Ann Plast Surg* 2007;59(2):137–42.
- [12] Coleman SR, Saboeiro AP. Primary breast augmentation with fat grafting. *Clin Plast Surg* 2015;42(3):301–6. vii.
- [13] Yang J, Zhou C, Fu J, Yang Q, He T, Tan Q, et al. In situ adipogenesis in biomaterials without cell seeds: current status and perspectives. *Front Cell Dev Biol* 2021;9:647149.
- [14] Wang C, Long X, Si L, Chen B, Zhang Y, Sun T, et al. A pilot study on ex vivo expanded autologous adipose-derived stem cells of improving fat retention in localized scleroderma patients. *Stem Cells Transl Med* 2021;10(8):1148–56.
- [15] Bora P, Majumdar AS. Adipose tissue-derived stromal vascular fraction in regenerative medicine: a brief review on biology and translation. *Stem Cell Res Ther* 2017;8(1):145.
- [16] Jiang W, Cai J, Guan J, Liao Y, Lu F, Ma J, et al. Characterized the adipogenic capacity of adipose-derived stem cell, extracellular matrix, and microenvironment with fat components grafting. *Front Cell Dev Biol* 2021;9:723057.
- [17] Park B, Kong JS, Kang S, Kim YW. The effect of epidermal growth factor on autogenous fat graft. *Aesthetic Plast Surg* 2011;35(5):738–44.
- [18] Camaj P, Seeliger H, Ischenko I, Krebs S, Blum H, De Toni EN, et al. EFEMP1 binds the EGF receptor and activates MAPK and Akt pathways in pancreatic carcinoma cells. *Biol Chem* 2009;390(12):1293–302.
- [19] Kendall RT, Feghali-Bostwick CA. Fibroblasts in fibrosis: novel roles and mediators. *Front Pharmacol* 2014;5:123.
- [20] Rhee S, Grinnell F. Fibroblast mechanics in 3D collagen matrices. *Adv Drug Deliv Rev* 2007;59(13):1299–305.
- [21] Sbarbati A, Accorsi D, Benati D, Marchetti L, Orsini G, Rigotti G, et al. Subcutaneous adipose tissue classification. *Eur J Histochem* 2010;54(4):e48.
- [22] Driskell RR, Watt FM. Understanding fibroblast heterogeneity in the skin. *Trends Cell Biol* 2015;25(2):92–9.
- [23] Ichim TE, O'heeron P, Kesari S. Fibroblasts as a practical alternative to mesenchymal stem cells. *J Transl Med* 2018;16(1):212.
- [24] Hofstatter EW, Horvath S, Dalela D, Gupta P, Chagpar AB, Wali VB, et al. Increased epigenetic age in normal breast tissue from luminal breast cancer patients. *Clin Epigenetics* 2018;10(1):112.
- [25] Wang JM, Gu Y, Pan CJ, Yin LR. Isolation, culture and identification of human adipose-derived stem cells. *Exp Ther Med* 2017;13(3):1039–43.
- [26] Du QC, Zhang DZ, Chen XJ, Lan-Sun G, Wu M, Xiao WL. The effect of p38MAPK on cyclic stretch in human facial hypertrophic scar fibroblast differentiation. *PLoS One* 2013;8(10):e75635.
- [27] Gluckman E, Broxmeyer HA, Auerbach AD, Friedman HS, Douglas GW, Devergie A, et al. Hematopoietic reconstitution in a patient with Fanconi's anemia by means of umbilical-cord blood from an HLA-identical sibling. *N Engl J Med* 1989;321(17):1174–8.
- [28] Cappellesso-Fleury S, Puissant-Lubrano B, Apoil PA, Titeux M, Winterton P, Casteilla L, et al. Human fibroblasts share immunosuppressive properties with bone marrow mesenchymal stem cells. *J Clin Immunol* 2010;30(4):607–19.
- [29] Ren D, Dai Y, Yang Q, Zhang X, Guo W, Ye L, et al. Wnt5a induces and maintains prostate cancer cells dormancy in bone. *J Exp Med* 2019;216(2):428–49.
- [30] Liu Y, Chen C, He H, Wang D, E L, Liu Z, et al. Lentiviral-mediated gene transfer into human adipose-derived stem cells: role of NELL1 versus BMP2 in osteogenesis and adipogenesis *in vitro*. *Acta Biochim Biophys Sin (Shanghai)* 2012;44(10):856–65.
- [31] Wu Y, Ou Y, Liao C, Liang S, Wang Y. High-throughput sequencing analysis of the expression profile of microRNAs and target genes in mechanical force-

- induced osteoblastic/cementoblastic differentiation of human periodontal ligament cells. *Am J Transl Res* 2019;11(6):3398–411.
- [32] Tateishi K, Ando W, Higuchi C, Hart DA, Hashimoto J, Nakata K, et al. Comparison of human serum with fetal bovine serum for expansion and differentiation of human synovial MSC: potential feasibility for clinical applications. *Cell Transplant* 2008;17(5):549–57.
- [33] Ma B, Li M, Fuchs S, Bischoff I, Hofmann A, Unger RE, et al. Short-term hypoxia promotes vascularization in co-culture system consisting of primary human osteoblasts and outgrowth endothelial cells. *J Biomed Mater Res A* 2020;108(1):7–18.
- [34] Haubner F, Muschter D, Pohl F, Schreml S, Prantl L, Gassner HG. A Co-culture model of fibroblasts and adipose tissue-derived stem cells reveals new insights into impaired wound healing after radiotherapy. *Int J Mol Sci* 2015;16(11):25947–58.
- [35] Carpino G, Cardinale V, Di Giamberardino A, Overi D, Donsante S, Colasanti T, et al. Thrombospondin 1 and 2 along with PEDF inhibit angiogenesis and promote lymphangiogenesis in intrahepatic cholangiocarcinoma. *6th75. J Hepatol*; 2021. p. 1377–86.
- [36] Kolpakov MA, Guo X, Rafiq K, Vlasenko L, Hooshdaran B, Seqqat R, et al. Loss of protease-activated receptor 4 prevents inflammation resolution and predisposes the heart to cardiac rupture after myocardial infarction. *Circulation* 2020;142(8):758–75.
- [37] Zheng L, Li Y, Geng F, Zheng S, Yan R, Han Y, et al. Using semi-quantitative dynamic contrast-enhanced magnetic resonance imaging parameters to evaluate tumor hypoxia: a preclinical feasibility study in a maxillofacial VX2 rabbit model. *Am J Transl Res* 2015;7(3):535–47.
- [38] Pu LLQ, Coleman SR, Cui X, Ferguson Jr REH, Vasconez HC. Autologous fat grafts harvested and refined by the Coleman technique: a comparative study. *Plast Reconstr Surg* 2008;122(3):932–7.
- [39] Zhang W, Fan W, Rachagani S, Zhou Z, Lele SM, Batra SK, et al. Comparative study of subcutaneous and orthotopic mouse models of prostate cancer: vascular perfusion, vasculature density, hypoxic burden and BB2r-targeting efficacy. *Sci Rep* 2019;9(1):11117.
- [40] Sijbesma JWA, Van Waarde A, Stegger L, Dierckx Rajo, Boersma HH, Slart Rhja. PET/CT imaging and physiology of mice on high protein diet. *Int J Mol Sci* 2021;22(6).
- [41] Liu R, Tang J, Xu Y, Dai Z. Bioluminescence imaging of inflammation in vivo based on bioluminescence and fluorescence resonance energy transfer using nanobubble ultrasound contrast agent. *ACS Nano* 2019;13(5):5124–32.
- [42] Van Heetvelde M, Van Bockstal M, Poppe B, Lambein K, Rosseel T, Atanesyan L, et al. Accurate detection and quantification of epigenetic and genetic second hits in BRCA1 and BRCA2-associated hereditary breast and ovarian cancer reveals multiple co-acting second hits. *Cancer Lett* 2018;425:125–33.
- [43] Huang H, Feng S, Zhang W, Li W, Xu P, Wang X, et al. Bone marrow mesenchymal stem cell-derived extracellular vesicles improve the survival of transplanted fat grafts. *Mol Med Rep* 2017;16(3):3069–78.
- [44] Shi J, Liang J, Guo B, Zhang Y, Hui Q, Chang P, et al. Adipose-derived stem cells cocultured with chondrocytes promote the proliferation of chondrocytes. *Stem Cells Int* 2017;2017:1709582.
- [45] Yan H, Mi X, Midgley AC, Du X, Huang Z, Wei T, et al. Targeted repair of vascular injury by adipose-derived stem cells modified with P-selectin binding peptide. *Adv Sci (Weinh)* 2020;7(11):1903516.
- [46] Pittenger MF, Mackay AM, Beck SC, Jaiswal RK, Douglas R, Mosca JD, et al. Multilineage potential of adult human mesenchymal stem cells. *Science* 1999;284(5411):143–7.
- [47] Ejaz A, Wu D, Kwan P, Meydani M. Curcumin inhibits adipogenesis in 3T3-L1 adipocytes and angiogenesis and obesity in C57/BL mice. *J Nutr* 2009;139(5):919–25.
- [48] Tang W, Song H, Cai W, Shen X. Real time monitoring of inhibition of adipogenesis and angiogenesis by (-)-epigallocatechin-3-Gallate in 3T3-L1 adipocytes and human umbilical vein endothelial cells. *Nutrients* 2015;7(10):8871–86.
- [49] Suga H, Eto H, Aoi N, Kato H, Araki J, Doi K, et al. Adipose tissue remodeling under ischemia: death of adipocytes and activation of stem/progenitor cells. *Plast Reconstr Surg* 2010;126(6):1911–23.
- [50] Wang J, Wu H, Zhao Y, Qin Y, Zhang Y, Pang H, et al. Extracellular vesicles from HIF-1 α -overexpressing adipose-derived stem cells restore diabetic wounds through accelerated fibroblast proliferation and migration. *Int J Nanomedicine* 2021;16:7943–57.
- [51] Junker JP, Lonnqvist S, Rakar J, Karlsson LK, Grenegard M, Kratz G. Differentiation of human dermal fibroblasts towards endothelial cells. *Differentiation* 2013;85(3):67–77.
- [52] Newman AC, Nakatsu MN, Chou W, Gershon PD, Hughes CC. The requirement for fibroblasts in angiogenesis: fibroblast-derived matrix proteins are essential for endothelial cell lumen formation. *Mol Biol Cell* 2011;22(20):3791–800.
- [53] Ejaz A, Hatzmann FM, Hammerle S, Ritthammer H, Mattesich M, Zwierzina M, et al. Fibroblast feeder layer supports adipogenic differentiation of human adipose stromal/progenitor cells. *Adipocyte* 2019;8(1):178–89.
- [54] Yoon JS, Lee HJ, Chae MK, Lee SY, Lee EJ. Cigarette smoke extract-induced adipogenesis in Graves' orbital fibroblasts is inhibited by quercetin via reduction in oxidative stress. *J Endocrinol* 2013;216(2):145–56.
- [55] Wei Z, Batagov AO, Schinelli S, Wang J, Wang Y, El Fatimy R, et al. Coding and noncoding landscape of extracellular RNA released by human glioma stem cells. *Nat Commun* 2017;8(1):1145.
- [56] Zhao J, Hu L, Liu J, Gong N, Chen L. The effects of cytokines in adipose stem cell-conditioned medium on the migration and proliferation of skin fibroblasts in vitro. *Biomed Res Int* 2013;2013:578479.
- [57] Rosen ED, Hsu CH, Wang X, Sakai S, Freeman MW, Gonzalez FJ, et al. C/EBP α induces adipogenesis through PPAR γ : a unified pathway. *Genes Dev* 2002;16(1):22–6.
- [58] Zhang S, Dong Z, Peng Z, Lu F. Anti-aging effect of adipose-derived stem cells in a mouse model of skin aging induced by D-galactose. *PLoS One* 2014;9(5):e97573.
- [59] Hu L, Yang G, Hagg D, Sun G, Ahn JM, Jiang N, et al. IGF1 promotes adipogenesis by a lineage bias of endogenous adipose stem/progenitor cells. *Stem Cells* 2015;33(8):2483–95.
- [60] Kolle SF, Fischer-Nielsen A, Mathiasen AB, Elberg JJ, Oliveri RS, Glovinski PV, et al. Enrichment of autologous fat grafts with ex-vivo expanded adipose tissue-derived stem cells for graft survival: a randomised placebo-controlled trial. *Lancet* 2013;382(9898):1113–20.
- [61] Swanson E. Prospective controlled study of buttock fat transfer using ultrasound and photographic measurements. *Plast Reconstr Surg Glob Open* 2016;4(5):e697.
- [62] Cetinkaya A, Devoto MH. Periocular fat grafting: indications and techniques. *Curr Opin Ophthalmol* 2013;24(5):494–9.
- [63] Bennett KG, Qi J, Kim HM, Hamill JB, Wilkins EG, Mehrara BJ, et al. Association of fat grafting with patient-reported outcomes in postmastectomy breast reconstruction. *JAMA Surg* 2017;152(10):944–50.
- [64] Billings Jr E, May Jr JW. Historical review and present status of free fat graft autotransplantation in plastic and reconstructive surgery. *Plast Reconstr Surg* 1989;83(2):368–81.
- [65] Bellini E, Grieco MP, Rapisio E. The science behind autologous fat grafting. *Ann Med Surg (Lond)* 2017;24:65–73.
- [66] Petrucelli N, Daly MB, Pal T. BRCA1- and BRCA2-associated hereditary breast and ovarian cancer [M]. In: Adam MP, Mirzaa GM, Pagon RA, et al., editors. *GeneReviews*(R). City. University of Washington; 1993. <http://www.ncbi.nlm.nih.gov/pubmed/20301425>.
- [67] Zhang L, Li Y, Gu Z, Wang Y, Shi M, Ji Y, et al. Resveratrol inhibits enterovirus 71 replication and pro-inflammatory cytokine secretion in rhabdomyosarcoma cells through blocking IKKs/NF-kappaB signaling pathway. *PLoS One* 2015;10(2):e0116879.
- [68] Busquets S, Ametller E, Fuster G, Oliván M, Raab V, Argiles JM, et al. Resveratrol, a natural diphenol, reduces metastatic growth in an experimental cancer model. *Cancer Lett* 2007;245(1–2):144–8.
- [69] Garvin S, Ollinger K, Dabrosin C. Resveratrol induces apoptosis and inhibits angiogenesis in human breast cancer xenografts in vivo. *Cancer Lett* 2006;231(1):113–22.
- [70] Lei S, Zheng R, Zhang S, Chen R, Sun K, et al. Global patterns of breast cancer incidence and mortality: a population-based cancer registry data analysis from 2000 to 2020. *Cancer Commun (Lond)* 2021;41(11):1183–94.
- [71] Ye Y, Dai Q, Qi H. A novel defined pyroptosis-related gene signature for predicting the prognosis of ovarian cancer. *Cell Death Discov* 2021;7(1):71.